

Networked Time Series Prediction with Incomplete Data

Yichen Zhu
zyc_ieee@sjtu.edu.cn
Shanghai Jiao Tong University
Shanghai, China

Mengtian Zhang
zhangmengtian@sjtu.edu.cn
Shanghai Jiao Tong University
Shanghai, China

Bo Jiang
bjiang@sjtu.edu.cn
Shanghai Jiao Tong University
Shanghai, China

Haiming Jin
jinhaiming@sjtu.edu.cn
Shanghai Jiao Tong University
Shanghai, China

Jianqiang Huang
jianqiang.jqh@gmail.com
Alibaba Damo Academy
Hangzhou, China

Xinbing Wang
xwang8@sjtu.edu.cn
Shanghai Jiao Tong University
Shanghai, China

ABSTRACT

A *networked time series (NETS)* is a family of time series on a given graph, one for each node. It has found a wide range of applications from intelligent transportation, environment monitoring to mobile network management. An important task in such applications is to predict the future values of a NETS based on its historical values and the underlying graph. Most existing methods require complete data for training. However, in real-world scenarios, it is not uncommon to have missing data due to sensor malfunction, incomplete sensing coverage, etc. In this paper, we study the problem of *NETS prediction with incomplete data*. We propose NETS-ImpGAN, a novel deep learning framework that can be trained on incomplete data with missing values in both history and future. Furthermore, we propose novel *Graph Temporal Attention Networks* by incorporating the attention mechanism to capture both inter-time series correlations and temporal correlations. We conduct extensive experiments on three real-world datasets under different missing patterns and missing rates. The experimental results show that NETS-ImpGAN outperforms existing methods except when data exhibit very low variance, in which case NETS-ImpGAN still achieves competitive performance.

KEYWORDS

networked time series, incomplete data, prediction, imputation

1 INTRODUCTION

A *networked time series (NETS)* is a family of time series on a given graph, one for each node [5]. Depending on the application, the underlying graph may encode spatial proximity, statistical dependency, or other contextual or structural information about the time series. As a versatile modeling tool, NETS have found a wide range of applications from intelligent transportation, environment monitoring to mobile network management.

An important task in such applications is to predict the future values of a NETS based on its historical values and the underlying graph. This has been studied extensively and many prediction methods have been proposed in various contexts; see [3, 5, 9, 11, 15, 22, 30, 34, 38, 39, 42, 44] and references therein. Most of these methods use deep learning and require complete data for training [3, 9, 11, 15, 22, 30, 34, 38, 39, 42]. However, in real-world scenarios, it is not uncommon to have missing data due to sensor malfunction, incomplete sensing coverage, etc. Simply removing all samples with missing data could lead to low data efficiency, as some observed data

will also be removed [1]. This motivates us to study the problem of *NETS prediction with incomplete data*.

This problem has been considered in the context of matrix completion. Dynamic Contextual Matrix Factorization (DCMF) [5] combines linear dynamic system and joint matrix factorization to impute missing data in a NETS. By treating the future as missing data, it can also be used for prediction [6]. As the model is always fitted to a single sample with no future data, it cannot benefit from training on multiple samples to learn more complex dependencies between history and future than the assumed linear system model.

A more recent work [44] proposes Recurrent Imputation based Heterogeneous Graph Convolution Network (RIHGCN). For training, each NETS sample is divided into history and future in the temporal dimension. RIHGCN first uses Graph Convolutional Network (GCN) [18] and Long Short-Term Memory (LSTM) [14] network to impute missing data in the history part, and then uses the completed history to predict the future. The two steps are trained jointly to mitigate the errors accumulated in the imputation step. However, RIHGCN still requires complete future data for supervision during training and does not provide a full solution to our problem.

Different from existing work, the goal of the present paper is to design a prediction framework for NETS that can learn complex dependencies from data with missing values in both history and future. A key challenge here is how to use incomplete future data to supervise the prediction. A simple adaptation of existing methods by computing the prediction loss only on observed future values can lead to inferior performance. Our solution is to learn the conditional distribution of the future with the observed values providing constraints on marginals. By supervision on distributions rather than individual values, we can more readily use observed values in different samples to guide the prediction.

More specifically, we reduce the prediction problem to a special type of imputation problem as in [6], and propose a novel framework called *Imputation Generative Adversarial Net (ImpGAN)* for its solution. ImpGAN has a generator that takes incomplete history and noise as input, and outputs complete samples including predicted future and imputed history. The complete samples are then properly masked to generate new fake incomplete samples, which the discriminator tries to distinguish from real incomplete samples. As such, ImpGAN is a generic framework for imputation and may be of independent interest.

Another challenge is to capture the inter-time series correlations and temporal correlations of incomplete NETS. Existing methods

typically use GCN [18] to capture inter-time series correlations, and variants of Convolutional Neural Network (CNN) [37] or Recurrent Neural Network (RNN) [32] to capture temporal correlations, e.g. [3, 9, 11, 15, 22, 30, 34, 38, 39, 42, 44]. However, these networks are not designed for incomplete data. When dealing with incomplete data, we typically fill missing values with random noise or constants so all samples have the same shape. As noted in [44], this may lead to inferior performance due to error accumulation. We note that the filled values and true observed values are of quite different natures and should be treated differently. Furthermore, the differential treatments should adapt to different samples as missing patterns vary. To address this challenge, we propose *Graph Temporal Attention Networks (GTANs)* by incorporating Graph Attention Network [36] and Self Attention [35]. Using GTANs to implement the generators and discriminators of ImpGAN, we obtain the full model named *Networked Time Series ImpGAN (NETS-ImpGAN)* for NETS prediction with incomplete data.

To summarize, we make the following contributions.

- We propose NETS-ImpGAN, a novel deep learning framework for NETS prediction with incomplete data. To the best of our knowledge, this is the first such framework that can be trained on incomplete data with missing values in both history and future.
- We propose GTANs to capture inter-time series correlations and temporal correlations of incomplete NETS. GTANs can adapt to different incomplete samples by incorporating the attention mechanism.
- We conduct extensive experiments on three real-world datasets under different missing patterns and missing rates. The experimental results show that NETS-ImpGAN outperforms existing methods except when data exhibit very low variance, in which case NETS-ImpGAN still achieves competitive performance.

2 RELATED WORK

NETS prediction. The problem of NETS prediction has been studied extensively in various contexts; see [3, 5, 9, 11, 15, 22, 30, 34, 38, 39, 42, 44] and references therein. Its extension to tensor-valued NETS has also been considered [6, 13, 16]. Most existing methods require complete data for training. They typically use GCN [18] to capture inter-time series correlations, and variants of CNN [37] or RNN [32] to capture temporal correlations [3, 9, 11, 15, 22, 30, 34, 38, 39, 42]. For the tensor-valued extension, [16] proposes Tensor GCN and Tensor RNN.

In contrast, there is limited literature on NETS prediction with incomplete data. DCMF [5] is a matrix factorization method for missing data imputation of NETS, which can also be used for prediction by treating the future as missing data. Its key assumptions are that a NETS and its associated graph have certain low-rank matrix representations, and that the temporal dynamics follows a first-order linear system. Facets [6] extends DCMF to tensor-valued NETS by using tensor decomposition instead of matrix factorization. Net-Dyna [13] further considers the case where the underlying graph is also incomplete. All three models are fitted to a single sample with no future data. Without explicit learning to predict the future, their predictive power relies critically on the strong and potentially restrictive assumption of linear system model. WDGTC [23] considers so-called weakly dependent modes in tensor completion.

Without a model for temporal dynamics, it lacks the ability to predict the future. RIHGCN [44] is a deep learning framework for NETS prediction. It first uses GCN [18] and LSTM [14] to impute missing data in the history, and then uses the completed history to predict the future. The imputation and prediction steps are trained jointly to mitigate error accumulation. RIHGCN also uses multiple graphs, static and dynamic, to capture dynamic inter-time series correlation. However, it requires complete future data for training.

In what follows, we review some imputation methods for other data types that can use incomplete data for supervision.

Multiple time series imputation. There are many methods for multiple time series imputation in the literature. They can also be used for prediction by treating the future as missing data. Among them, BRITS and E²GAN [7, 25, 26] can use incomplete data for supervision. BRITS [7] imputes missing values using a bidirectional RNN [33] with a temporal decay factor. It minimizes the reconstruction errors on observed entries and forces the imputed values of missing entries to be consistent in both directions. E²GAN [25, 26] is a GAN-based framework where the generator imputes missing values and the discriminator tries to distinguish completed data from incomplete real data. To capture temporal correlations of incomplete data, the generator and discriminator use a novel GRUI cell, which incorporates a temporal decay factor in Gated Recurrent Unit (GRU) [8]. Both BRITS and E²GAN take into account correlations between all the time series in the imputation process, effectively treating multiple time series as a special NETS with a complete underlying graph. As such, they cannot exploit the additional information provided by the graph of a general NETS.

General data imputation. There are several general imputation methods [20, 21, 41] that can use incomplete data for supervision. GAIN [41] adapts the GAN architecture [12], in which the generator imputes missing data, a hint generator provides partial information of missing entries to the discriminator, and the discriminator distinguishes between the observed entries and the imputed entries. MisGAN [20] uses a GAN [12] to learn the complete data distribution from incomplete data and then uses the learned complete distribution to supervise the imputation. P-VAE [27], MIWAE [28] and P-BiGAN [21] extends VAE [17], IWAE [4] and BiGAN [10] respectively to an encoding-decoding framework that models the distribution of incomplete data together with its latent representation. They conduct case studies on image data by adopting 2-dimensional CNN-based models [37] to capture the spatial correlations of grid-structured data, but cannot be directly applied to NETS. As shown in previous works, these methods have close performance. We will make a comparison to MisGAN, which shares some similarities with ImpGAN.

Compared to the existing models, the proposed NETS-ImpGAN can use incomplete future data for supervision and adapt to different incomplete samples when capturing both the inter-time series correlations and temporal correlations.

3 PROBLEM DEFINITION

3.1 Background and Notations

A networked time series (NETS) is a family of time series defined on a given graph. Let $\mathcal{G} = (\mathcal{V}, \mathcal{E})$ be an undirected graph with node set $\mathcal{V} = \{1, 2, \dots, V\}$ and edge set $\mathcal{E} \subset \mathcal{V} \times \mathcal{V}$. A NETS on \mathcal{G} over

timestamps $\mathcal{T} = \{1, 2, \dots, T\}$ is $(\mathbf{X}, \mathcal{G})$, where $\mathbf{X} = (X_{v,t}) \in \mathbb{R}^{V \times T}$ is a matrix whose entry $X_{v,t}$ is the value at time t of the time series on node $v \in \mathcal{V}$. Since we only consider the case where the graph \mathcal{G} is fixed and known, we will refer to a NETS by \mathbf{X} for simplicity. It is understood that the underlying \mathcal{G} is given.

In the presence of missing data, only part of \mathbf{X} is observed. A binary mask $\mathbf{M} = (M_{v,t}) \in \{0, 1\}^{V \times T}$ indicates which entries of \mathbf{X} are observed: $M_{v,t} = 1$ if $X_{v,t}$ is observed, and $M_{v,t} = 0$ if $X_{v,t}$ is missing. The complementary mask $\bar{\mathbf{M}} \in \{0, 1\}^{V \times T}$ is defined by $\bar{M}_{v,t} = 1 - M_{v,t}, \forall v, t$. With a slight abuse of notation, we also regard \mathbf{M} and $\bar{\mathbf{M}}$ as the index sets of the observed and missing entries of \mathbf{X} , respectively. Then we can denote the observed data by $\mathbf{X}_{\mathbf{M}} = \{X_{v,t} \mid (v,t) \in \mathbf{M}\}$ and the missing data by $\mathbf{X}_{\bar{\mathbf{M}}} = \{X_{v,t} \mid (v,t) \in \bar{\mathbf{M}}\}$. We consider the case where it is known which entries are observed. Thus an incomplete data sample is given by $(\mathbf{X}_{\mathbf{M}}, \mathbf{M})$. An incomplete dataset consists of N incomplete data samples, denoted by $\mathcal{D} = \{(\mathbf{X}_{\mathbf{M}^{(i)}}^h, \mathbf{M}^{(i)})\}_{i=1,2,\dots,N}$.

Following [24], we model the generative process of incomplete data as follows. A complete data sample \mathbf{X} is first drawn from the complete data distribution $p(\mathbf{X})$. Given \mathbf{X} , a mask sample \mathbf{M} is then drawn from the conditional mask distribution $p(\mathbf{M} \mid \mathbf{X})$. The resulted incomplete data sample $(\mathbf{X}_{\mathbf{M}}, \mathbf{M})$ follows the distribution

$$p(\mathbf{X}_{\mathbf{M}}, \mathbf{M}) = \int p(\mathbf{X})p(\mathbf{M} \mid \mathbf{X})d\mathbf{X}_{\bar{\mathbf{M}}}.$$

We focus on the Missing Completely At Random (MCAR) case [24] where the mask \mathbf{M} is independent of the underlying complete data \mathbf{X} , i.e., $p(\mathbf{M} \mid \mathbf{X}) = p(\mathbf{M})$. Our proposed framework can be easily generalized to the Missing At Random (MAR) case [24] where \mathbf{M} only depends on the observed data $\mathbf{X}_{\mathbf{M}}$, i.e., $p(\mathbf{M} \mid \mathbf{X}) = p(\mathbf{M} \mid \mathbf{X}_{\mathbf{M}})$.

3.2 Problem Statement

Given the incomplete history $(\mathbf{X}_{\mathbf{M}^h}^h, \mathbf{M}^h)$ of a NETS over T^h timestamps, our task is to predict the future values \mathbf{X}^f over the next T^f timestamps. More specifically, we seek a prediction function g_{pred} that takes $(\mathbf{X}_{\mathbf{M}^h}^h, \mathbf{M}^h) \sim p(\mathbf{X}_{\mathbf{M}^h}^h, \mathbf{M}^h)$ as input and outputs the desired future \mathbf{X}^f .

We allow g_{pred} to be random to accommodate multiple prediction [24], where multiple predicted values are given to reflect the uncertainty. Ideally we would like the predicted values to follow the conditional distribution of the future given the history, i.e.

$$\mathbf{X}^f = g_{\text{pred}}(\mathbf{X}_{\mathbf{M}^h}^h, \mathbf{M}^h) \sim p(\mathbf{X}^f \mid \mathbf{X}_{\mathbf{M}^h}^h, \mathbf{M}^h).$$

When a single predicted value is desired, we can use a summary statistic such as mean of multiple predicted values. Note that g_{pred} may depend on the underlying graph \mathcal{G} , which is part of the input.

The predictor g_{pred} will be trained on an incomplete dataset whose samples have missing values in both history and future. A sample in the dataset is $(\mathbf{X}_{\mathbf{M}^h}^h, \mathbf{M}^h; \mathbf{X}_{\mathbf{M}^f}^f, \mathbf{M}^f)$, where $(\mathbf{X}_{\mathbf{M}^f}^f, \mathbf{M}^f)$ is the incomplete future, and $\mathbf{M}^f \in \{0, 1\}^{V \times T^f}$ the corresponding mask. Note that the challenge here is how to use the incomplete future $(\mathbf{X}_{\mathbf{M}^f}^f, \mathbf{M}^f)$ to supervise the complete prediction \mathbf{X}^f .

4 METHODOLOGIES

In this section, we begin with a reduction of the prediction problem to an imputation problem in Section 4.1. Then we introduce the proposed framework in Section 4.2 and the training of the framework in Section 4.3. Finally, we present the design of the neural networks for the modules of the framework in Section 4.4.

4.1 Problem Reduction

We address the prediction problem in Section 3.2 by reducing it to an imputation problem as follows. We first regard history and future as a whole sample $(\mathbf{X}_{\mathbf{M}}, \mathbf{M})$, where $T = T^h + T^f$, $\mathcal{T} = \mathcal{T}^h \cup \mathcal{T}^f$, $\mathbf{X} = \mathbf{X}^h \parallel \mathbf{X}^f$, $\mathbf{M} = \mathbf{M}^h \parallel \mathbf{M}^f$, and \parallel stands for concatenation along the temporal dimension. Next, we introduce a new mask $\mathbf{M}^* = \mathbf{M}^h \parallel \mathbf{O}^f \in \{0, 1\}^{V \times T}$, which is the concatenation of \mathbf{M}^h and an all-zero mask \mathbf{O}^f of size $V \times T^f$ along the temporal dimension. By the all-zero \mathbf{O}^f in \mathbf{M}^* , we treat the future as missing data. In this way, $\mathbf{X}_{\mathbf{M}^h}^h = \mathbf{X}_{\mathbf{M}^*}$, i.e., $(\mathbf{X}_{\mathbf{M}^*}, \mathbf{M}^*)$ provides the same information as $(\mathbf{X}_{\mathbf{M}^h}^h, \mathbf{M}^h)$ does. Then we can impute the missing data $\mathbf{X}_{\bar{\mathbf{M}}^*}$ from incomplete data $(\mathbf{X}_{\mathbf{M}^*}, \mathbf{M}^*)$. The imputed $\mathbf{X}_{\bar{\mathbf{M}}^*}$ contains both imputed history $\mathbf{X}_{\mathbf{M}^h}^h$ and predicted future \mathbf{X}^f . As a result, instead of learning g_{pred} , we can learn a random function g_{imp} such that

$$g_{\text{imp}}(\mathbf{X}_{\mathbf{M}^*}, \mathbf{M}^*) \sim p(\mathbf{X}_{\bar{\mathbf{M}}^*} \mid \mathbf{X}_{\mathbf{M}^*}, \mathbf{M}^*).$$

In the learning process of g_{imp} , the incomplete dataset \mathcal{D} is available, which has missing values in both history and future. Instead of supervising only on the future part, we can supervise on both history and future, i.e., using incomplete history and future $(\mathbf{X}_{\mathbf{M}}, \mathbf{M})$ to supervise the missing history and the whole future $\mathbf{X}_{\bar{\mathbf{M}}^*}$. Note that the input to g_{imp} is $(\mathbf{X}_{\mathbf{M}^*}, \mathbf{M}^*)$, while $(\mathbf{X}_{\mathbf{M}}, \mathbf{M})$ is used for supervision, which further contains the incomplete future. In this way, we can use incomplete future to supervise the prediction. In the next part, we will introduce how to realize such supervision.

4.2 Framework

For the random function g_{imp} , by the reparameterization trick, we can instead use a deterministic g_{imp} that takes some random noise \mathbf{Z} as an additional input. Thus the goal is to learn a function $g_{\text{imp}}(\mathbf{X}_{\mathbf{M}^*}, \mathbf{M}^*, \mathbf{Z})$ such that

$$g_{\text{imp}}(\mathbf{X}_{\mathbf{M}^*}, \mathbf{M}^*, \mathbf{Z}) \sim p(\mathbf{X}_{\bar{\mathbf{M}}^*} \mid \mathbf{X}_{\mathbf{M}^*}, \mathbf{M}^*).$$

We adopt Generative Adversarial Net (GAN) [12] to learn g_{imp} for its high sampling efficiency and propose a deep learning framework named *Networked Time Series Imputation GAN (NETS-ImpGAN)*. The architecture of NETS-ImpGAN is shown in Figure 1.

First, we learn the mask distribution $p(\mathbf{M})$. Since mask \mathbf{M} is observed in \mathcal{D} , we adopt a standard GAN $(G_m(\omega), D_m(\mathbf{M}))$ to learn $p(\mathbf{M})$, in which mask generator $G_m(\omega)$ takes random noise $\omega \sim p_\omega$ as input and generates fake mask $\bar{\mathbf{M}}$, and mask discriminator $D_m(\mathbf{M})$ takes as input either the real mask \mathbf{M} from \mathcal{D} or the fake mask $\bar{\mathbf{M}}$ generated by G_m and distinguishes between them. Here $\mathbf{M} = \mathbf{M}^h \parallel \mathbf{M}^f$ indicates partially observable future.

Next, we realize g_{imp} by the imputation generator $G_i(\mathbf{X}, \mathbf{M}^*, \mathbf{Z})$ that aims to learn the conditional distribution of missing data $p(\mathbf{X}_{\bar{\mathbf{M}}^*} \mid \mathbf{X}_{\mathbf{M}^*}, \mathbf{M}^*)$. Here $\mathbf{M}^* = \mathbf{M}^h \parallel \mathbf{O}^f$ indicates fully missing

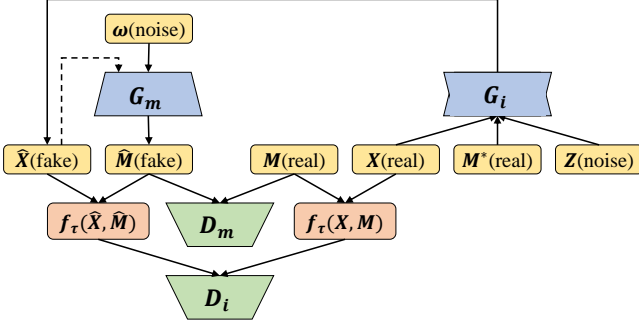


Figure 1: Architecture of NETS-ImpGAN

future. The construction of G_i is

$$G_i(\mathbf{X}, \mathbf{M}^*, \mathbf{Z}) = \mathbf{X} \odot \mathbf{M}^* + \hat{G}_i(\mathbf{X} \odot \mathbf{M}^* + \mathbf{Z} \odot \bar{\mathbf{M}}^*) \odot \bar{\mathbf{M}}^*,$$

where $\mathbf{Z} \sim p_{\mathbf{Z}}$ is random noise of size $V \times T$, \odot stands for element-wise multiplication, and \hat{G}_i is a function that has input and output of the same size. In this paper, \hat{G}_i is implemented by the neural network introduced in Section 4.4. Though we have \mathbf{X} in this matrix expression of G_i , the missing data $\mathbf{X}_{\bar{M}^*}$ is not required, since the masked form $\mathbf{X} \odot \mathbf{M}^*$ retains the observed data \mathbf{X}_{M^*} and masks the missing data $\mathbf{X}_{\bar{M}^*}$.

We use a second masked form $\mathbf{X} \odot \mathbf{M}^*$ outside of \hat{G}_i to retain the observed data. The output of G_i , denoted by $\hat{\mathbf{X}}$, is regarded as the imputed data, which consists of both imputed history and predicted future. Note that we discard the information about \mathbf{M}^* in $\hat{\mathbf{X}}$. As a result, if G_i captures the distribution $p(\mathbf{X}_{\bar{M}^*} | \mathbf{X}_{M^*}, \mathbf{M}^*)$, $\hat{\mathbf{X}}$ will follow the distribution

$$p(\mathbf{X}) = \int p(\mathbf{X}_{M^*}, \mathbf{M}^*) p(\mathbf{X}_{\bar{M}^*} | \mathbf{X}_{M^*}, \mathbf{M}^*) d\mathbf{M}^*.$$

In order to train the imputation generator G_i , we need to use the incomplete data $(\mathbf{X}_M, \mathbf{M})$ in \mathcal{D} to supervise the complete imputed data $\hat{\mathbf{X}}$. [20] learns the complete data distribution $p(\mathbf{X})$ under the supervision of $(\mathbf{X}_M, \mathbf{M})$ and use the learned complete data distribution to supervise $\hat{\mathbf{X}}$. However, the biased learned complete data distribution is regarded as ground truth, which results in error accumulation, as demonstrated in Section 5.8.

We overcome this issue by converting $\hat{\mathbf{X}}$ to incomplete data, which can be directly supervised by the incomplete data in \mathcal{D} . In order to use the incomplete future $(\mathbf{X}_{M^f}^f, \mathbf{M}^f)$ for supervision, we convert $\hat{\mathbf{X}} = \hat{\mathbf{X}}^h \parallel \hat{\mathbf{X}}^f$ to incomplete data that also has partially observable future. Specifically, we generate a new mask $\hat{\mathbf{M}} = \hat{\mathbf{M}}^h \parallel \hat{\mathbf{M}}^f$ by G_m and obtain the corresponding incomplete data sample $(\hat{\mathbf{X}}_{\hat{\mathbf{M}}}^h, \hat{\mathbf{M}}^h, \hat{\mathbf{X}}_{\hat{\mathbf{M}}^f}^f, \hat{\mathbf{M}}^f)$, which can be supervised by $(\mathbf{X}_M, \mathbf{M}) = (\mathbf{X}_{M^h}^h, \mathbf{M}^h, \mathbf{X}_{M^f}^f, \mathbf{M}^f)$. Note that the mask $\mathbf{M}^* = \mathbf{M}^h \parallel \mathbf{O}^f$ fed into G_i makes the whole future missing, but the mask $\mathbf{M} = \mathbf{M}^h \parallel \mathbf{M}^f$ used for supervision indicates partially observable future.

Since neural networks generally take fixed-shaped arrays as input, we cannot directly feed incomplete data $(\mathbf{X}_M, \mathbf{M})$ into the imputation discriminator D_i . Instead, we re-mask \mathbf{X} and $\hat{\mathbf{X}}$ with \mathbf{M} and $\hat{\mathbf{M}}$ respectively by the masking operator [20] defined as

$$f_\tau(\mathbf{X}, \mathbf{M}) = \mathbf{X} \odot \mathbf{M} + \tau \bar{\mathbf{M}},$$

which essentially retains the observed data and fills in the missing data entries with a constant τ . We set $\tau = 0$ in this paper. Though we have \mathbf{X} in this matrix expression of $f_\tau(\mathbf{X}, \mathbf{M})$, the missing data $\mathbf{X}_{\bar{M}}$ is not required, since the missing entries are filled with τ .

Finally, we have the imputation discriminator $D_i(f_\tau(\mathbf{X}, \mathbf{M}))$ distinguish between $f_\tau(\mathbf{X}, \mathbf{M})$ and $f_\tau(\hat{\mathbf{X}}, \hat{\mathbf{M}})$, which plays the role of supervision. In this way, we can use the available incomplete data to supervise the training of G_i . As proved in [20], D_i does not need to know the value and positions of τ .

Note that, for different incomplete data samples, the corresponding conditional distributions of the missing data are different, i.e., we need to learn a set of conditional distributions. Here we learn this set of distributions in an amortized manner [17]. That is, we take advantage of the high representation capability of neural network to represent all these distributions with one specific set of network parameters. In this way, there is no need to learn for each distribution respectively, and much training cost can be saved.

Since we focus on the MCAR case, mask generator $G_m(\omega)$ only takes random noise ω as input. To generalize to the MAR case, G_m can additionally take $\hat{\mathbf{X}}$ as input to model the dependence of mask \mathbf{M} on the underlying \mathbf{X} , as shown by the dotted line in Figure 1.

If we ignore the separation of history and future when learning $g_{\text{imp}}(\mathbf{X}_{M^*}, \mathbf{M}^*)$, we can simply regard \mathbf{M}^* as a general mask \mathbf{M} and generalize $g_{\text{imp}}(\mathbf{X}_{M^*}, \mathbf{M}^*)$ to $g_{\text{imp}}(\mathbf{X}_M, \mathbf{M})$. In this way, NETS-ImpGAN is a generic imputation framework of independent interest and can be applied to some other tasks.

4.3 Training

In the training phase, following Wasserstein GAN [2] for its high training stability, we define the loss functions as follows:

$$\begin{aligned} \mathcal{L}_m(D_m, G_m) &= \mathbb{E}[D_m(\mathbf{M})] - \mathbb{E}[D_m(G_m(\omega))], \\ \mathcal{L}_i(D_i, G_i, G_m) &= \mathbb{E}[D_i(f_\tau(\mathbf{X}, \mathbf{M}))] \\ &\quad - \mathbb{E}[D_i(f_\tau(G_i(\mathbf{X}, \mathbf{M}^*, \mathbf{Z}), G_m(\omega)))] \\ &\quad + \beta \mathbb{E} \|\hat{G}_i(\mathbf{X}, \mathbf{M}^*, \mathbf{Z}) \odot \mathbf{M}^* - \mathbf{X} \odot \mathbf{M}^*\|_1, \end{aligned}$$

where the expectations are taken over $(\mathbf{X}, \mathbf{M}) \sim p_{\mathcal{D}}$, $\omega \sim p_\omega$ and $\mathbf{Z} \sim p_{\mathbf{Z}}$, $p_{\mathcal{D}}$ is the underlying real distribution of \mathcal{D} , $\|\cdot\|_1$ stands for L_1 -norm, and β is the trade-off parameter of the L_1 -norm loss. We find that forcing the output of \hat{G}_i to have the same observed data as the input can improve the imputation performance, thus we add an additional reconstruction loss in the form of L_1 -norm. Note that we want the whole predicted future to be random. The reconstruction loss is only computed on the history part, since reconstruction loss on the future will force part of the future to be deterministic. Based on the loss functions, we define the optimization objectives of the generators and discriminators as follows:

$$\min_{G_m} \max_{D_m \in \mathcal{F}_m} \mathcal{L}_m(D_m, G_m),$$

$$\min_{G_i} \max_{D_i \in \mathcal{F}_i} \mathcal{L}_i(D_i, G_i, G_m),$$

where \mathcal{F}_m and \mathcal{F}_i are the families of 1-Lipschitz functions for D_m and D_i respectively.

4.4 Graph Temporal Attention Networks

In order to capture the inter-time series correlations and temporal correlations of incomplete NETS, we design *Graph Temporal Attention Networks (GTANs)* for the generators and the discriminators of NETS-ImpGAN. Specifically, we propose *Graph Temporal Attention U-Net (GTA U-Net)* for the imputation generator G_i and neural networks with similar building blocks for the other modules. In what follows, we first focus on the architecture of GTA U-Net and then the others. The architecture of GTA U-Net is shown in Figure 2.

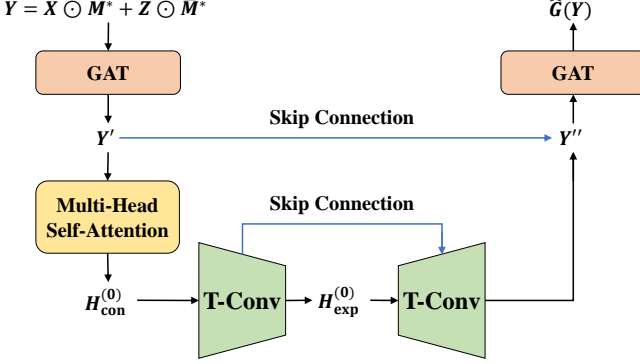


Figure 2: Architecture of GTA U-Net

The input to GTA U-Net is $X \odot M^* + Z \odot \bar{M}^*$, which introduces random noise to the data propagated through GTA U-Net. Since the observed values and the random noise are of quite different natures and the positions of them are possibly different in different incomplete samples as missing patterns vary, the neural networks need to adapt to these different samples in forward propagation. However, neural networks with static network weights [22, 30, 34, 38, 39, 42, 44] keep the same propagation for different samples. In order to overcome this issue, we incorporate attention mechanism from both the graph perspective and the temporal perspective.

Similar to U-Net [31], GTA U-Net has a U-shaped structure, which consists of a contracting encoding path (left side) and an expansive decoding path (right side). We use this structure to first extract a lower-dimensional representation of the input incomplete data and then recover the complete data from this representation. Along the encoding path, the input first goes through a layer of Graph Attention Network (GAT) [36], then a layer of Multi-Head Self-Attention [35] and finally a stack of Temporal Convolution (T-Conv). Along the decoding path, data goes through these layers symmetrically in the reverse order.

4.4.1 Graph Attention Network. We use Graph Attention Network (GAT) [36] to capture the inter-time series correlations. GAT incorporates attention mechanism into the graph neural network to realize adaptive node feature propagation.

The input to the GAT layer is $Y = X \odot M^* + Z \odot \bar{M}^*$. The graph attention operation is defined as

$$Y'_{i,t} = \alpha_{i,i,t} \theta Y_{i,t} + \sum_{j \in \mathcal{N}(i)} \alpha_{i,j,t} \theta Y_{j,t}, \quad t = 1, 2, \dots, T,$$

where $Y_{i,t} \in \mathbb{R}$ and $Y'_{i,t} \in \mathbb{R}$ are the input and output value on node i at timestamps t , $\mathcal{N}(i)$ is the one-hop neighborhood of node

i , $\theta \in \mathbb{R}$ is the training parameter. Note that the graph attention operation is decoupled for different timestamps t , thus the values at different timestamps can be propagated concurrently. The attention coefficient $\alpha_{i,j,t}$ is computed as

$$\alpha_{i,j,t} = \frac{\exp(\text{LeakyReLU}(\mathbf{a}^\top [\theta Y_{i,t} \parallel \theta Y_{j,t}]))}{\sum_{k \in \mathcal{N}(i) \cup \{i\}} \exp(\text{LeakyReLU}(\mathbf{a}^\top [\theta Y_{i,t} \parallel \theta Y_{k,t}]))},$$

where \parallel stands for concatenation, and $\mathbf{a} \in \mathbb{R}^2$ is the training parameter. Since the attention coefficient depends on the node values, GAT can adaptively propagate the node values.

The GAT layer is followed by an activation layer. We denote the output of the activation layer by $\mathbf{H} = \sigma(Y') \in \mathbb{R}^{V \times T}$, where σ stands for the activation function.

4.4.2 Multi-Head Self-Attention. We use Multi-Head Self-Attention [35] to capture the temporal correlations. Self-Attention mechanism builds representation subspaces based on the data features to realize adaptive propagation along the temporal dimension.

The input to the Multi-Head Self-Attention layer is \mathbf{H} . Multi-Head Self-Attention consists of multiple heads. The i -th head is defined as follows. First, three vectors are computed: the query $\mathbf{Q}_i = \mathbf{H}^\top \mathbf{W}^{Q_i} \in \mathbb{R}^{T \times d_q}$, the key $\mathbf{K}_i = \mathbf{H}^\top \mathbf{W}^{K_i} \in \mathbb{R}^{T \times d_k}$ with $d_k = d_q$ and the value $\mathbf{V}_i = \mathbf{H}^\top \mathbf{W}^{V_i} \in \mathbb{R}^{T \times d_v}$. \mathbf{W}^{Q_i} , \mathbf{W}^{K_i} and \mathbf{W}^{V_i} are the parameter matrices. The output of the i -th head is computed by

$$\text{head}_i = \text{softmax} \left(\frac{\mathbf{Q}_i \mathbf{K}_i^\top}{\sqrt{d_k}} \right) \mathbf{V}_i,$$

where the superscript \top stands for transpose. Multi-Head Self-Attention jointly attends to input from different representation subspaces to obtain more informative representation by

$$\text{MultiHead} = \mathbf{W}^O \text{Concat}(\text{head}_1, \dots, \text{head}_h)^\top,$$

where $\text{Concat}(\cdot)$ stands for concatenation along the second dimension, and $\mathbf{W}^O \in \mathbb{R}^{V \times h d_v}$ is the parameter matrix. Since the attention matrix $\mathbf{Q}_i \mathbf{K}_i^\top$ is computed based on the input \mathbf{H} , Self-Attention can adaptively correlate each timestamp in the output to all the timestamps in the input from a global point of view.

4.4.3 Temporal Convolution. Different from Multi-Head Self-Attention, we use Temporal Convolution (T-Conv) to capture the temporal correlations in a local view of the neighboring timestamps. We also extract lower-dimensional representation of the input data.

We use 1-dimensional CNN along the temporal dimension to reduce or increase the dimensionality of data along the temporal dimension. Specifically, each T-Conv layer in the contracting path reduces the temporal length of data by half, and each one in the expansive path doubles it. There are L layers along the contractive path and also L layers along the expansive path. We denote the output of Multi-Head Self-Attention by $\mathbf{H}_{\text{con}}^{(0)} \in \mathbb{R}^{V \times T}$ to indicate that it is the input to the first layer of Temporal Convolution along the contractive path. The l -th contracting T-Conv layer is

$$\mathbf{H}_{\text{con}}^{(l)} = \text{Conv1d}(\mathbf{H}_{\text{con}}^{(l-1)}, \text{stride} = 2),$$

where $\mathbf{H}_{\text{con}}^{(l-1)} \in \mathbb{R}^{V \times T/2^{l-1}}$ and $\mathbf{H}_{\text{con}}^{(l)} \in \mathbb{R}^{V \times T/2^l}$ are the input and output, and $\text{Conv1d}(\cdot, \text{stride} = 2)$ stands for 1-dimensional CNN with stride 2. The outputs of the expansive T-Conv layers have the same temporal length as the symmetric ones along the contracting

path. In addition, following the practice of U-Net [31], we also adopt skip connections, as shown by the blue curves. Skip connection is used to preserve the border information, i.e., information at the beginning and end timestamps, since the border information tends to be lost after every convolution operation. The input to the first expansive convolutional layer is $\mathbf{H}_{\text{exp}}^{(0)} = \mathbf{H}_{\text{con}}^{(L)} \in \mathbb{R}^{V \times T/2^L}$, and the l -th expansive T-Conv layer is

$$\mathbf{H}_{\text{exp}}^{(l)} = \text{DeConv1d}([\mathbf{H}_{\text{exp}}^{(l-1)}, \mathbf{H}_{\text{con}}^{(L-l+1)}], \text{stride} = 2),$$

where $\mathbf{H}_{\text{exp}}^{(l-1)} \in \mathbb{R}^{V \times T/2^{L-l+1}}$ and $\mathbf{H}_{\text{exp}}^{(l)} \in \mathbb{R}^{V \times T/2^{L-l}}$ are the input and output, $[\cdot, \cdot]$ stands for concatenation along the feature dimension, and $\text{DeConv1d}(\cdot, \text{stride} = 2)$ stands for 1-dimensional de-convolutional layer with stride 2. Though the input to each expansive T-Conv layer has 2-dimensional feature due to concatenation, the output still has only 1-dimensional feature.

By using convolutional structures to capture the temporal correlations, we also avoid the issue of error accumulation, which recurrent structures usually suffer from. In this way, we reach higher stability in multi-step prediction, as demonstrated in Section 5.6.

The output of the L -th expansive T-Conv layer has the same size as $\mathbf{Y}' \in \mathbb{R}^{V \times T}$. Though the feature map of the graph is preserved, skip connection still works by transmitting information directly from the contracting path to the expansive path. As a result, the input to the final GAT layer is $\mathbf{Y}'' = [\mathbf{H}_{\text{exp}}^{(L)}, \mathbf{Y}'] \in \mathbb{R}^{V \times T \times 2}$. The output of the final GAT layer is

$$\hat{G}_i(\mathbf{Y}) = \sigma^o(\text{GAT}(\mathbf{Y}'')),$$

where GAT stands for the operation of a GAT layer, and σ^o is the activation function for the output. Though \mathbf{Y}'' has 2-dimensional feature due to concatenation, the output of the final GAT layer $\text{GAT}(\mathbf{Y}'') \in \mathbb{R}^{V \times T}$ has only 1-dimensional feature.

4.4.4 Mask Generator and the Discriminators. The building blocks of mask generator G_m , mask discriminator D_m and imputation discriminator D_i are similar to those of GTA U-Net.

The architecture of mask generator G_m is shown in Figure 3(a). The random noise ω first goes through a Fully-Connected (FC) layer, which is used to reshape the input data to the desired shape. Then the reshaped data goes through several layers of T-Conv and a layer of GAT, which is the same as the expansive path of GTA U-Net, except that there is no skip connection. When capturing the inter-time series correlations, we also use GAT to compute dynamic graph weights, since no static weight is provided in \mathcal{G} .

The architecture of the discriminators D_m and D_i are the same, as shown in Figure 3(b). The input data goes through a layer of GAT, a layer of Multi-Head Self-Attention and several layers of T-Conv, which is the same as the contracting path of GTA U-Net. Finally, the data goes through a Fully-Connected (FC) layer, which is used to reshape the data to a scalar. The output scalar stands for the judgement of the discriminator on how real the input data is. When capturing the inter-time series correlations, we also use GAT to adapt to different incomplete samples, since the constants τ and the observed data are also of different natures.

5 EXPERIMENTS

In this section, we evaluate the proposed model NETS-ImpGAN. First, we describe the datasets in Section 5.1. Next, we introduce

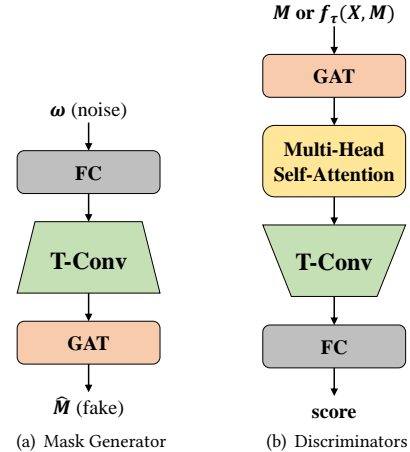


Figure 3: Mask generator and the discriminators

the baseline models, the missingness setup, the evaluation metrics and the implementation details in Sections 5.2 to 5.5. Finally, we present and analyze the experiment results in Sections 5.6 to 5.8.

5.1 Datasets

We evaluate NETS-ImpGAN by a case study on traffic scenario. The following three large-scale public real-world datasets are used in the experiments.

Hangzhou Metro Passenger Flow (HZ-Flow). HZ-Flow [30] is a collection of passenger outbound flow from 81 metro stations in Hangzhou, China, within every 10 minutes from Jan. 1st to Jan. 25th, 2019. This data set is collected from around 70 million automated fare collection records. In the associated graph, nodes represent the metro stations, and edges are constructed based on the pairwise passenger transition probability as follows. In the presence of data missingness, we first delete the automated fare collection records that correspond to the missing part of all the incomplete data samples and then follow [30] to compute the transition probability matrix with the remaining records. An undirected edge is added between a pair of nodes if at least one of the transition probability between them is no less than 0.02.

Los Angeles Highway Speed (LA-Speed). LA-Speed [22] is a collection of average speed recorded by 207 loop detectors on the highway network of Los Angeles, USA, within every 5 minutes from Mar. 1st to June 30th, 2012. In the associated graph, nodes represent the loop detectors, and edges are constructed based on the pairwise highway network distance as follows. We follow [22] to process the pairwise distance with Gaussian kernel. A pair of nodes are connected by an undirected edge if their processed distance is at least 0.1.

Beijing Taxi Flow (BJ-Flow). The city of Beijing, China, is divided into a 32×32 grid. BJ-Flow [43] is a collection of taxi outbound flow from the 1024 grid cells within every 30 minutes in the following four time intervals: July 1st - Oct. 30th, 2013, Mar. 1st - June 30th, 2014, Mar. 1st - June 30th, 2015, Nov. 1st, 2015 - Apr. 10th, 2016. We treat the grid as a special case of graph, where

nodes represent the grid cells, and each cell is connected to the four neighboring cells on the north, south, east and west.

5.2 Baseline Methods

We compare NETS-ImpGAN with the following baselines, including both simple ones and state of the art. For a fair comparison, we only consider models that do not require complete data for training.

- **Mean.** For every data sample, Mean predicts the missing entries with the mean value of the observed entries.
- **Temporal Linear Extrapolation (TLE).** For every data sample, TLE predicts each missing entry with the linear function that passes through its last two observed historical entries on the same node.
- **Last Observation (LO).** For every data sample, LO predicts each missing entry with the last-observed historical value on the same node.
- **BRITS [7].** BRITS uses a bidirectional RNN [33] with a temporal decay factor to impute missing data in multiple time series. It minimizes the reconstruction errors on observed entries and forces the imputed values of missing entries to be consistent in both directions. It does not exploit the information provided by the graph of a NETS.
- **E²GAN [25, 26].** E²GAN is a GAN-based framework to impute missing values in multiple time series. The generator imputes missing values and the discriminator tries to distinguish completed data from incomplete real data. It does not exploit the information provided by the graph of a NETS.
- **DCMF [5].** DCMF combines linear dynamic system and joint matrix factorization to impute missing data in a NETS. The model is fitted to a single sample with no future data and its predictive power relies critically on the assumption of linear system model.

For TLE and LO, Mean is used if the required values are missing. For BRITS, E²GAN and DCMF, we use them for prediction by treating the future as missing data.

We make clear the differences between NETS-ImpGAN and the baselines with respect to (1) supervision with incomplete future, (2) capturing inter-time series correlations and (3) capturing temporal correlations in Table 1.

Table 1: Differences between NETS-ImpGAN and baselines

	Supervision	Graph	Temporal
Mean	×	×	×
TLE	×	×	√
LO	×	×	√
BRITS	√	×	√
E ² GAN	√	×	√
DCMF	×	√	√
NETS-ImpGAN	√	√	√

5.3 Missingness Setup

We manually mask the complete datasets and use the resulted incomplete datasets for evaluation. The performance is evaluated under four missing patterns. We evaluate under low, medium and high missing rates of 25%, 50% and 75% and also very low missing

rates of 2%, 4%, 6%, 8% and 10%. The design of the missing patterns are described as follows, where missing rate is denoted by r .

- **Random (Random).** In every data sample, values on all nodes at all timestamps are independently randomly missing with a probability of r .
- **Single Block of Fixed Shape (SF-Block).** In every data sample, the values on $\lfloor V\sqrt{r} \rfloor$ nodes at randomly selected $\lfloor T\sqrt{r} \rfloor$ consecutive timestamps are missing. The nodes are selected by running breadth-first traversal from a random node until desired number of nodes are traversed. The missing rate may not be exactly r due to possible rounding.
- **Single Block of Variable Shape (SV-Block).** In every data sample, the values on N_v nodes at randomly selected N_t consecutive timestamps are missing, where N_v and N_t are uniformly randomly drawn from $[l_v, u_v]$ and $[l_t, u_t]$. The nodes are selected in the same way as in SF-Block. In this paper, we set $l_v = \lfloor V/4 \rfloor$, $u_v = \lfloor 3V/4 \rfloor$, $l_t = \lfloor T/4 \rfloor$ and $u_t = \lfloor 3T/4 \rfloor$. The average missing rate is around 25%.
- **Multiple Blocks of Variable Shape (MV-Block).** In every data sample, more than one blocks are missing. In each of the blocks, the values on N_v nodes at randomly selected N_t consecutive timestamps are missing, where N_v and N_t are uniformly randomly drawn from $[l_v, u_v]$ and $[l_t, u_t]$. The nodes are selected in the same way as in SF-Block. The number of blocks is $\lfloor \frac{VT}{(l_v+u_v)(l_t+u_t)/4} \rfloor$. In this paper, we set $l_v = 1$, $u_v = 7$, $l_t = 1$ and $u_t = 3$. The blocks are selected independently, and thus the missing rate may not be exactly r due to possible overlapping of the blocks.

We evaluate point missingness under Random and block missingness under SF-Block, SV-Block and MV-Block. For block missingness, we evaluate single or multiple block of fixed or variable shape.

5.4 Evaluation Metrics

The appropriate evaluation metric may depend on the specific application scenario and/or user preference. Here we consider three metrics, Mean Absolute Error (MAE), Root Mean Square Error (RMSE) and Mean Absolute Percentage Error (MAPE). MAE and RMSE are used to measure absolute error, while MAPE is used to measure percentage error. Since we have learned a distribution of the future, we have the flexibility to optimize the prediction according to a given metric. Specifically, when the metrics are MAE and RMSE, we use the empirical median and mean, respectively, of multiple predicted values sampled from the imputation generator G_i . When MAPE is the metric, we solve an empirical MAPE minimization problem by quantile regression [19] to obtain the optimal predicted values. Since DCMF and E²GAN also have distributions, we do the same optimization for them.

5.5 Implementation Details

The proposed model is implemented in Python with the PyTorch library. We use 90% of the samples for training, 5% for validation and 5% for testing. The batch size is set to be 64. Training of the model takes 1000 epochs. In the training process, we use the Adam optimizer and set the learning rate to be 0.0001. The trade-off parameter β in Section IV.C is set to be 10. The noise ω fed into the mask generator is a 128-dimensional vector. The Multi-Head Self-Attention modules all have 3 heads. The Temporal Convolution

modules all have kernel of size 3×3 and stride 2, and the number of channels doubles along the contracting path and halves along the expansive path.

In data preprocessing, we observe that the ranges of value on different nodes vary greatly and thus apply Min-Max normalization to scale the data to $[-1, 1]$ for every node respectively. The metrics are computed with the data rescaled to the original range.

A data sample is composed of $T = 16$ timestamps. The former 8 corresponds to history, and the latter 8 corresponds to future. Missingness are set up respectively for the history and future.

In the imputation generator G_i , $L = 3$ T-Conv layers are used along the contractive and the expansive path respectively. LeakyReLU function is used for all but the last activation layer, and tanh function is used for the last activation layer to make the range of the generated data consistent with that of the normalized real data.

In the training phase, we follow the common practice that alternatively optimizes the discriminators for 5 epochs and the generators for 1 epoch. In the testing phase, we randomly generate 10 samples by G_i to calculate the predictors as specified in Section 5.4.

5.6 Prediction Performance

In this subsection, we evaluate the prediction performance by comparing NETS-ImpGAN with the baseline models on the three datasets under the four missing patterns and the eight levels of missing rates. Due to space limit, we only show the results under missing rate of 25%, and those under the other missing rates are similar. The performance of single prediction is shown in Figure 4.

From Figure 4, NETS-ImpGAN achieves the best performance on HZ-Flow and BJ-Flow under all the missing patterns, especially the general pattern MV-Block. On LA-Speed, LO achieves the best performance, and NETS-ImpGAN achieves comparable performance.

Mean, TLE and LO have strong assumptions on the data distribution. Mean assumes value has low variance along both the graph and temporal dimensions, TLE assumes values follow a linear function along the temporal dimension, and LO assumes values are stable along the temporal dimension. Since these assumptions do not hold in most settings, these models have poor performance in most setting, except that LO achieves the best performance on LA-Speed, the reason for which will be discussed later. BRITS and E²GAN capture the temporal correlations with no assumption and thus can achieve better performance than Mean and TLE, while they cannot exploit the underlying graph. DCMF can further exploit the underlying graph, leading to better performance than BRITS and E²GAN. However, DCMF does not use the incomplete future, which results in worse performance than NETS-ImpGAN.

Then we discuss the performance of NETS-ImpGAN and LO on LA-Speed. LO achieves better performance than NETS-ImpGAN, since the data distribution along the temporal dimension is highly stable, which is consistent with the assumption of LO. We verify the influence of temporal stability on the performance of NETS-ImpGAN and LO as follows. We disrupt the temporal stability by adding randomness to the original data and use the disrupted data as ground truth for training. Specifically, a zero-mean Gaussian random scalar is added to each data point. Since the ranges of values on different nodes vary greatly, the standard derivation is determined with proportion γ to the range of original data on each

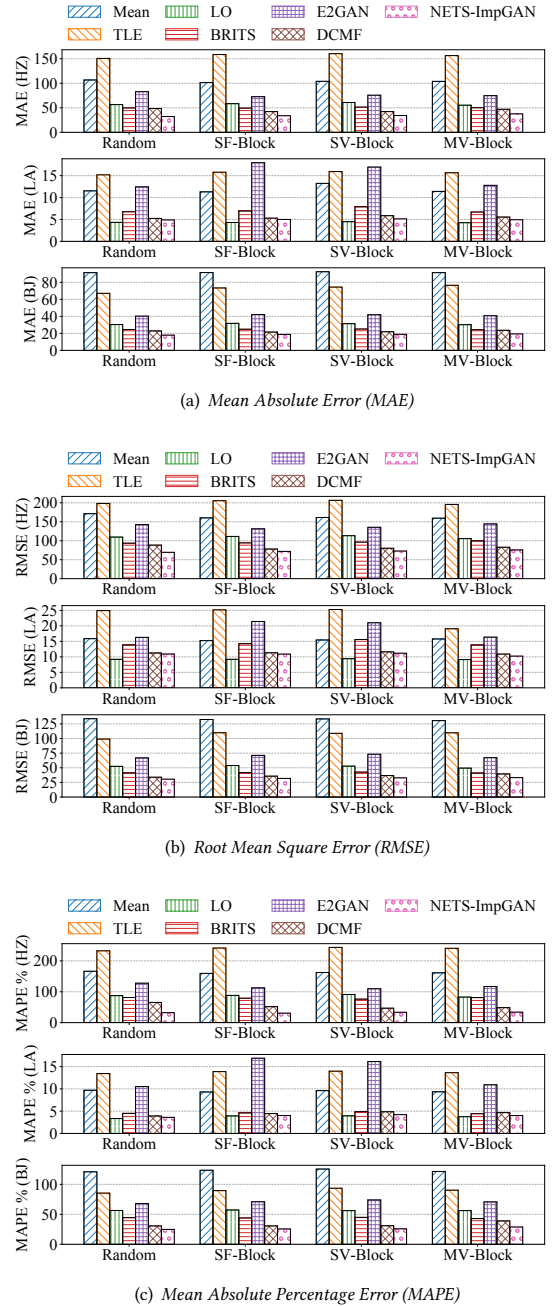


Figure 4: Prediction performance under missing rate of 25%

node respectively. For example, supposing the values on some node range from 0 to 100, $\gamma = 0.05$ results in a Gaussian random scalar with zero mean and standard derivation of 5. We set γ from 0.05 to 0.25 with a step of 0.05. The larger γ is, the stronger the disruption is, and the lower the temporal stability is.

We evaluate the performance of NETS-ImpGAN and LO on the disrupted datasets. The performance of single prediction under

MV-Block and missing rate of 25% is shown in Figure 5, and those under the other settings are similar. From Figure 5, NETS-ImpGAN drops slower than LO and outperforms LO when γ reaches a certain level, which demonstrates that LO highly relies on the assumption of temporal stability, and NETS-ImpGAN has stronger robustness to unstable temporal dynamics.

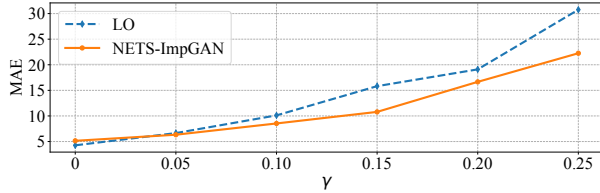


Figure 5: Prediction with decreasing temporal stability

Next, we investigate the performance with increasing missing rate. The performance of single prediction on HZ-Flow under MV-Block is shown in Figure 6, and those under the other settings are similar. Since Mean, TLE and E^2 GAN have much poorer performance than the others, we omit them in the plot for better visualization and easy comparison.

From Figure 6, all the models degrade with the increase of missing rate, since the proportion of available information becomes smaller and smaller. Among all the models, the performance of NETS-ImpGAN drops slowly, suggesting that NETS-ImpGAN is robust to high missing rate. LO and BRITS have poor performance, since the proportion of available information along the temporal dimension decreases faster than in both graph and temporal dimensions. DCMF can exploit information along both dimensions, but assumes the temporal dynamics follows linear dynamic systems. Compared to the baseline models, NETS-ImpGAN can capture both the correlations among time series and the temporal correlations and has no assumption on the temporal dynamics, thus achieving robustness to high missing rate.

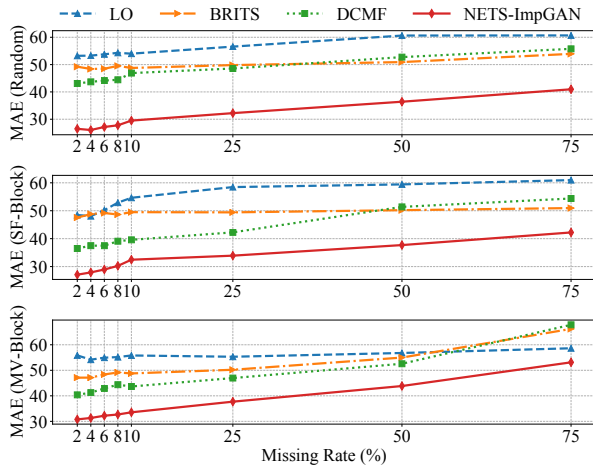


Figure 6: Prediction with increasing missing rate

We also investigate the multi-step prediction performance. The performance of single prediction on HZ-Flow under MV-Block and missing rate of 25% is shown in Figure 7, and those under the other settings are similar. We also omit the performance of Mean, TLE and E^2 GAN. Figure 7 shows NETS-ImpGAN achieves the highest stability as time steps goes further. Since LO assumes temporal stability and DCMF assumes linear dynamic systems, which may not hold, they result in poor stability. BRITS uses recurrent structures that potentially suffer from error accumulation, which also leads to poor stability. Compared to the baseline models, NETS-ImpGAN capture the temporal correlations with convolutional structures that do not have the issue of error accumulation and thus achieves the highest stability.

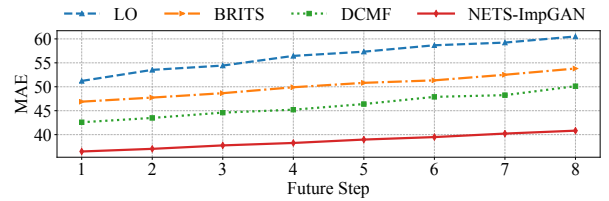


Figure 7: Multi-step prediction

5.7 Comparison with Two-Phase Prediction

In order to address the issue of low data efficiency when removing the samples with missing data, an intuitive way is to first impute the incomplete data and then use the imputed data to train a prediction that requires complete data for training. However, this way could lead to error accumulation, since biased imputed values are regarded as ground truth by the prediction model. In this subsection, we study the performance of two-phase prediction. As we mentioned in Section 4.2, NETS-ImpGAN can also be used for imputation. We first verify the imputation performance of NETS-ImpGAN and then show the performance of two-phase prediction where NETS-ImpGAN is used to impute the incomplete data.

In order to evaluate the imputation performance, we compare NETS-ImpGAN to Mean, BRITS, E^2 GAN, DCMF and three more imputation methods as follows.

- **Neighborhood Average (NA)**. For every data sample, NA imputes each missing entry with the mean of its observed one-hop neighbors on the underlying graph at the same timestamp.
- **Temporal Linear Interpolation (TLI)**. For every data sample, TLI imputes each missing entry with the mean of its last-observed historical and first-observed future entries on the same node.
- **WDGTC [23]**. WDGTC is a tensor completion method for so-called weakly dependent data. Without a model for temporal dynamics, it can only be used for imputation but not prediction.

For NA and TLI, Mean is used if the required values are missing.

Since we will investigate the performance of multiple imputation on the downstream prediction task, we first introduce the metric that measures the results of multiple imputation. We adopt Wasserstein Distance (WD) [40] to measure distributional error between the imputed dataset and the real dataset. Since distribution

is implicitly modeled by GAN [12], WD is approximated by the empirical distribution of the real dataset and the generated dataset that consists of finite number of samples generated by the imputation generator G_i .

The performance of single and multiple imputation under missing rate of 25% are shown in Figure 8, and those under the other missing rates are similar.

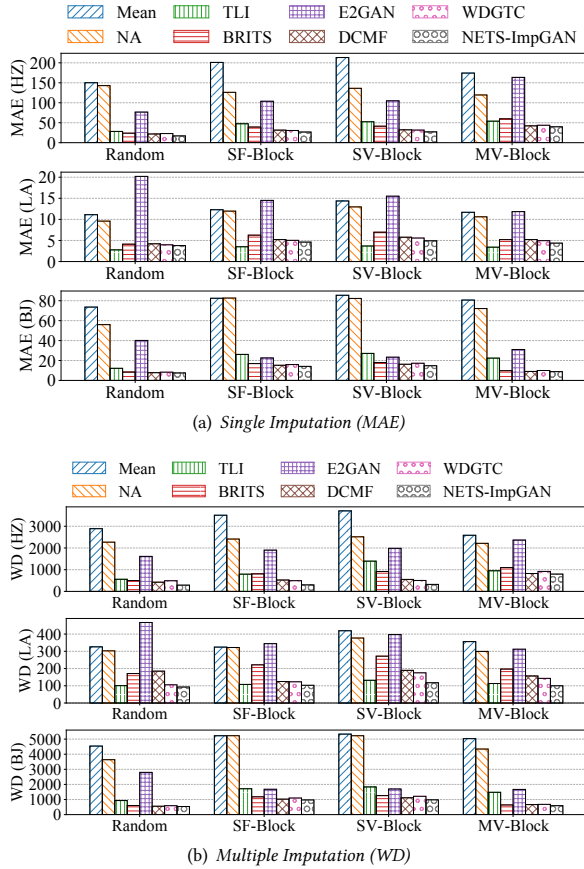


Figure 8: Imputation performance under missing rate of 25%

From Figure 8, in single imputation, NETS-ImpGAN achieves the best performance on HZ-Flow and BJ-Flow and comparable performance on LA-Speed; in multiple imputation, NETS-ImpGAN achieves the best performance on all the datasets.

We also show the performance with increasing missing rate. The performance of single imputation on HZ-Flow under MV-Block is shown in Figure 9, and those under the other settings are similar. We also omit the performance of Mean, NA and E²GAN. From Figure 9, NETS-ImpGAN is also robust to high missing rate.

Then we compare two-phase prediction to end-to-end prediction by NETS-ImpGAN. We first use NETS-ImpGAN and the baseline models to impute the incomplete dataset and then use the imputed complete dataset to train a GTA U-Net model for prediction. For NETS-ImpGAN, we conduct both single imputation with mean

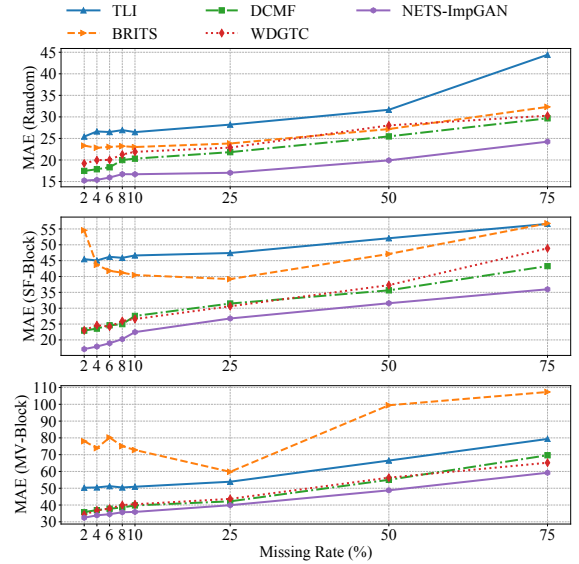


Figure 9: Imputation with increasing missing rate

value and multiple imputation. The prediction performance on HZ-Flow under missing rate of 25% is shown in Figure 10. Imputing with [model] is denoted by [model]+. We also omit the performance of Mean, NA and E²GAN. For the fixed prediction model, NETS-ImpGAN achieves the best downstream prediction performance among all the imputation models, which verifies the imputation performance of NETS-ImpGAN. Comparing single and multiple imputation, we find that multiple imputation can achieve slightly better performance. A possible reason is that the multiple imputation samples can help the downstream prediction model better understand the uncertainty in temporal dynamics. However, even if we use NETS-ImpGAN for imputation in two-phase prediction, two-phase prediction still has worse performance than end-to-end prediction. Note that we specially use GTA U-Net as the prediction model to guarantee that the two-phase prediction using NETS-ImpGAN for imputation and GTA U-Net for prediction has the same capability of capturing the correlations among time series and the temporal correlations as the end-to-end NETS-ImpGAN. Thus the results proves that end-to-end prediction can achieve better performance by overcoming the issue of error accumulation in two-phase prediction.

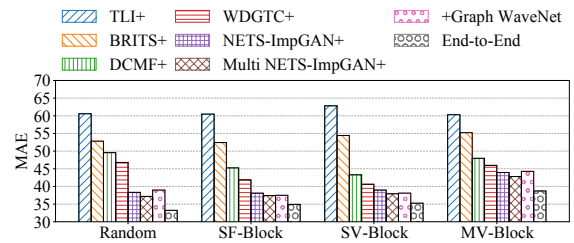


Figure 10: Two-phase vs. end-to-end prediction

We also fix the imputation model to be NETS-ImpGAN and then use GTA U-Net and Graph WaveNet [39] as the prediction model, respectively. Predicting with Graph WaveNet is denoted by +Graph WaveNet. As shown in Figure 10, the prediction performance by Graph WaveNet is close to GTA U-Net, and is also worse than end-to-end prediction, which further proves the existence of error accumulation in two-phase prediction.

5.8 Comparison with Model Variants

We first verify the efficacy of the components of the GTAN by comparing NETS-ImpGAN with the following variants.

- GTAN-w/o-G. In this variant, we remove the GAT modules in all the generators and discriminators.
- GTAN-w/o-T. In this variant, we remove the Multi-Head Self-Attention modules and T-Conv modules in all the generators and discriminators.
- GTAN-w/o-A. In this variant, we remove the attention mechanism in all the generators and discriminators. Along the graph dimension, we replace GAT with GraphConv [29], which is designed for graph with static weights. We preserve the passenger transition probability and highway network distance as graph weight for HZ-Flow and LA-Speed respectively and set the weights of all edges to be 1 for BJ-Flow. Along the temporal dimension, we remove the Multi-Head Self-Attention modules in all the generators and discriminators.

The performance of single prediction on HZ-Flow under missing rate of 25% is shown in Figure 11. From Figure 11, GTAN with all the components achieves the best performance, which proves the efficacy of all the components. Among the variants, GTAN-w/o-T has much worse performance than the others, suggesting the significance of capturing temporal correlations. Removing the graph component or the attention mechanism also have an influence on the performance.

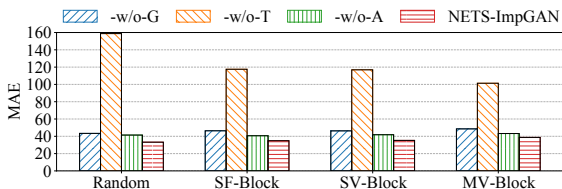


Figure 11: NETS-ImpGAN vs. ablated variants

We also verify the issue of error accumulation in MisGAN, as mentioned in Section 4.2. In order to make a fair comparison, we adopt the same GTANs inside the generators and discriminators of MisGAN, denoted by NETS-MisGAN, to guarantee that NETS-ImpGAN and NETS-MisGAN have the same capability of capturing the correlations among time series and the temporal correlations. We compare NETS-ImpGAN with the following variants.

- NETS-MisGAN-FakeData. In this variant, we train NETS-MisGAN in the same way as MisGAN. That is, samples from the learned complete data distribution are fed into the imputation discriminator D_i , and D_i regards these samples as ground truth.

- NETS-MisGAN-RealData. In this variant, we do not learn the complete data distribution but directly feed the complete ground truth samples to D_i , which can also be regarded as training NETS-ImpGAN with zero missing rate.
- NETS-ImpGAN-RealMask. In this variant, we do not learn the mask distribution but directly use mask samples from the underlying mask distribution in place of those generated by G_m .

Note that the only difference between NETS-MisGAN-FakeData and NETS-MisGAN-RealData is that D_i receives biased ground truth samples in NETS-MisGAN-FakeData and unbiased ones in NETS-MisGAN-RealData.

The performance of single prediction on HZ-Flow under missing rate of 25% is shown in Figure 12. NETS-MisGAN-RealData achieves the best performance, since complete ground truth is only available in NETS-MisGAN-RealData but not in the others. Compared to NETS-MisGAN-FakeData, the performance improvement of NETS-MisGAN-RealData proves the existence of error accumulation, and the performance improvement of NETS-ImpGAN demonstrates that NETS-ImpGAN can overcome the issue of error accumulation. The learned mask distribution can also lead to error accumulation in both NETS-ImpGAN and MisGAN, since samples generated by G_m are regarded as ground truth when fed into D_i . We verify such error accumulation by the variant NETS-ImpGAN-RealMask. From Figure 12, the difference between NETS-ImpGAN and NETS-ImpGAN-RealMask is almost negligible. The reason is that the binary mask distribution is relatively easy to learn, and the learned mask distribution can be highly close to the ground truth distribution.

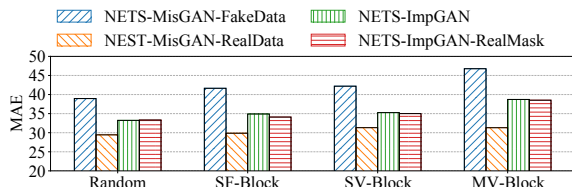


Figure 12: NETS-ImpGAN vs. MisGAN

6 CONCLUSION

In this paper, we study the problem of *NETS prediction with incomplete data*. In order to learn complex dependencies from data with missing values in both history and future, we use incomplete future for supervision from the distributional perspective. Specifically, we reduce the prediction problem to an imputation problem and propose NETS-ImpGAN, a novel deep learning framework that can be trained on incomplete data with missing values in both history and future. Furthermore, in order to overcome the issue of error accumulation when capturing the inter-time series correlations and temporal correlations, we propose novel *Graph Temporal Attention Networks (GTANs)* by incorporating the attention mechanism. The experimental results on three real-world datasets under different missing patterns and missing rates demonstrate that the proposed NETS-ImpGAN outperforms existing methods except when data exhibit very low variance, in which case NETS-ImpGAN still achieves competitive performance.

REFERENCES

- [1] Paul D. Allison. 2001. *Missing Data*. Sage Publications, USA.
- [2] Martin Arjovsky, Soumith Chintala, and Leon Bottou. 2017. Wasserstein Generative Adversarial Networks. In *Proceedings of the 34th International Conference on Machine Learning*. Sydney, Australia, 214–223.
- [3] Lei Bai, Lina Yao, Salil S. Kanhere, Xianzhi Wang, and Quan Z. Sheng. 2019. STG2Seq: Spatial-Temporal Graph to Sequence Model for Multi-step Passenger Demand Forecasting. In *Proceedings of the 28th International Joint Conference on Artificial Intelligence*. Macao, China, 1981–1987.
- [4] Yuri Burda, Roger B. Grosse, and Ruslan Salakhutdinov. 2016. Importance Weighted Autoencoders. In *4th International Conference on Learning Representations*. San Juan, Puerto Rico.
- [5] Yongjie Cai, Hanghang Tong, Wei Fan, and Ping Ji. 2015. Fast Mining of a Network of Coevolving Time Series. In *Proceedings of the 2015 SIAM International Conference on Data Mining*. Vancouver, Canada, 298–306.
- [6] Yongjie Cai, Hanghang Tong, Wei Fan, Ping Ji, and Qing He. 2015. Facets: Fast Comprehensive Mining of Coevolving High-order Time Series. In *Proceedings of the 21th ACM SIGKDD International Conference on Knowledge Discovery and Data Mining*. Sydney, Australia, 79–88.
- [7] Wei Cao, Dong Wang, Jian Li, Hao Zhou, Lei Li, and Yitan Li. 2018. BRITS: Bidirectional Recurrent Imputation for Time Series. In *Advances in Neural Information Processing Systems*. Montreal, Canada, 6775–6785.
- [8] Kyunghyun Cho, Bart van Merriënboer, Caglar Gulcehre, Dzmitry Bahdanau, Fethi Bougares, Holger Schwenk, and Yoshua Bengio. 2014. Learning Phrase Representations using RNN Encoder-Decoder for Statistical Machine Translation. In *Proceedings of the 2014 Conference on Empirical Methods in Natural Language Processing*. Doha, Qatar, 1724–1734.
- [9] Zulong Diao, Xin Wang, Dafang Zhang, Yingru Liu, Kun Xie, and Shaoyao He. 2019. Dynamic Spatial-Temporal Graph Convolutional Neural Networks for Traffic Forecasting. In *The 33rd AAAI Conference on Artificial Intelligence*. Honolulu, USA, 890–897.
- [10] Jeff Donahue, Philipp Krahenbuhl, and Trevor Darrell. 2017. Adversarial Feature Learning. In *International Conference on Learning Representations*. Toulon, France.
- [11] Xu Geng, Yaguang Li, Leye Wang, Lingyu Zhang, Qiang Yang, Jieping Ye, and Yan Liu. 2019. Spatiotemporal Multi-Graph Convolution Network for Ride-Hailing Demand Forecasting. In *The 33rd AAAI Conference on Artificial Intelligence*. Honolulu, USA, 3656–3663.
- [12] Ian Goodfellow, Jean Pouget-Abadie, Mehdi Mirza, Bing Xu, David Warde-Farley, Sherilj Ozair, Aaron Courville, and Yoshua Bengio. 2014. Generative Adversarial Nets. In *Advances in Neural Information Processing Systems*. Montreal, Canada, 2672–2680.
- [13] Hairi, Hanghang Tong, and Lei Ying. 2019. NetDyna: Mining Networked Coevolving Time Series with Missing Values. In *2019 IEEE International Conference on Big Data*. Los Angeles, USA, 503–512.
- [14] Sepp Hochreiter and Jürgen Schmidhuber. 1997. Long Short-Term Memory. *Neural Computation* 9, 8 (1997), 1735–1780.
- [15] Rongzhou Huang, Chuyin Huang, Yubao Liu, Genan Dai, and Weiyang Kong. 2020. LSGCN: Long Short-Term Traffic Prediction with Graph Convolutional Networks. In *Proceedings of the 29th International Joint Conference on Artificial Intelligence*. Virtual Event, 2355–2361.
- [16] Baoyu Jing, Hanghang Tong, and Yada Zhu. 2021. Network of Tensor Time Series. In *The Web Conference*. Ljubljana, Slovenia, 2425–2437.
- [17] Diederik P. Kingma and Max Welling. 2014. Auto-Encoding Variational Bayes. In *International Conference on Learning Representations*. Banff, Canada.
- [18] Thomas N. Kipf and Max Welling. 2017. Semi-Supervised Classification with Graph Convolutional Networks. In *International Conference on Learning Representations*. Toulon, France.
- [19] Roger Koenker and Kevin F. Hallock. 2001. Quantile Regression. *Journal of economic perspectives* 15, 4 (2001), 143–156.
- [20] Steven Cheng-Xian Li, Bo Jiang, and Benjamin Marlin. 2019. Learning from Incomplete Data with Generative Adversarial Networks. In *Proceedings of the 7th International Conference on Learning Representations*. New Orleans, USA.
- [21] Steven Cheng-Xian Li and Benjamin Marlin. 2020. Learning from Irregularly-Sampled Time Series: A Missing Data Perspective. In *Proceedings of the 37th International Conference on Machine Learning*. Virtual Event, 5937–5946.
- [22] Yaguang Li, Rose Yu, Cyrus Shahabi, and Yan Liu. 2018. Diffusion Convolutional Recurrent Neural Network: Data-Driven Traffic Forecasting. In *Proceedings of the 6th International Conference on Learning Representations*. Vancouver, Canada.
- [23] Ziyue Li, Nurettin Dorukhan Sergin, Hao Yan, Chen Zhang, and Fugee Tsung. 2020. Tensor Completion for Weakly-Dependent Data on Graph for Metro Passenger Flow Prediction. In *The 34th AAAI Conference on Artificial Intelligence*. New York, USA, 4804–4810.
- [24] Roderick J. A. Little and Donald B. Rubin. 1986. *Statistical Analysis with Missing Data*. John Wiley & Sons, Inc., USA.
- [25] Yonghong Luo, Xiangrui Cai, Ying Zhang, Jun Xu, and Xiaojie Yuan. 2018. Multivariate Time Series Imputation with Generative Adversarial Networks. In *Advances in Neural Information Processing Systems*. Montreal, Canada, 1596–1607.
- [26] Yonghong Luo, Ying Zhang, Xiangrui Cai, and Xiaojie Yuan. 2019. E²GAN: End-End Generative Adversarial Network for Multivariate Time Series Imputation. In *Proceedings of the 28th International Joint Conference on Artificial Intelligence*. Macao, China, 3094–3100.
- [27] Chao Ma, Sebastian Tschitschek, Konstantina Palla, Jose Miguel Hernandez-Lobato, Sebastian Nowozin, and Cheng Zhang. 2019. EDDI: Efficient Dynamic Discovery of High-Value Information with Partial VAE. In *Proceedings of the 36th International Conference on Machine Learning*. Long Beach, USA, 4234–4243.
- [28] Pierre-Alexandre Mattei and Jes Frelsen. 2019. MIWAE: Deep Generative Modelling and Imputation of Incomplete Data Sets. In *Proceedings of the 36th International Conference on Machine Learning*. Long Beach, USA, 4413–4423.
- [29] Christopher Morris, Martin Ritzert, Matthias Fey, William L. Hamilton, Jan Eric Lenssen, Gaurav Rattan, and Martin Grohe. 2019. Weisfeiler and Leman Go Neural: Higher-Order Graph Neural Networks. In *The 33rd AAAI Conference on Artificial Intelligence*. Honolulu, USA, 4602–4609.
- [30] Junjie Ou, Jiahui Sun, Yichen Zhu, Haiming Jin, Yijuan Liu, Fan Zhang, Jianqiang Huang, and Xinbing Wang. 2020. STP-TrellisNets: Spatial-Temporal Parallel TrellisNets for Metro Station Passenger Flow Prediction. In *Proceedings of the 29th ACM International Conference on Information and Knowledge Management*. Virtual Event, Ireland, 1185–1194.
- [31] Olaf Ronneberger, Philipp Fischer, and Thomas Brox. 2015. U-Net: Convolutional Networks for Biomedical Image Segmentation. In *Medical Image Computing and Computer-Assisted Intervention*. Munich, Germany, 234–241.
- [32] David E. Rumelhart, Geoffrey E. Hinton, and Ronald J. Williams. 1986. Learning Representations by Back-Propagating Errors. *Nature* 323 (1986), 1476–4687. Issue 6088.
- [33] Mike Schuster and Kuldip K. Paliwal. 1997. Bidirectional recurrent neural networks. *IEEE Transactions on Signal Processing* 45, 11 (1997), 2673–2681.
- [34] Feiyang Sun, Pinghui Wang, Junzhou Zhao, Nuo Xu, Juxiang Zeng, Jing Tao, Kaikai Song, Chao Deng, John C.S. Lui, and Xiaohong Guan. 2021. Mobile Data Traffic Prediction by Exploiting Time-Evolving User Mobility Patterns. *IEEE Transactions on Mobile Computing* 20 (2021), 1–14.
- [35] Ashish Vaswani, Noam Shazeer, Niki Parmar, Jakob Uszkoreit, Llion Jones, Aidan N. Gomez, Lukasz Kaiser, and Illia Polosukhin. 2017. Attention is All You Need. In *Advances in Neural Information Processing Systems*. Long Beach, USA, 5998–6008.
- [36] Petar Velickovic, Guillem Cucurull, Arantxa Casanova, Adriana Romero, Pietro Lio, and Yoshua Bengio. 2018. Graph Attention Networks. In *International Conference on Learning Representations*. Vancouver, Canada.
- [37] Alexander H. Waibel, Toshiyuki Hanazawa, Geoffrey E. Hinton, Kiyohiro Shikano, and Kevin J. Lang. 1989. Phoneme Recognition Using Time-Delay Neural Networks. *IEEE Transactions on Acoustics, Speech, and Signal Processing* 37 (1989), 328–339.
- [38] Tyler Wilson, Pang-Ning Tan, and Lifeng Luo. 2018. A Low Rank Weighted Graph Convolutional Approach to Weather Prediction. In *2018 IEEE International Conference on Data Mining*. Singapore, 627–636.
- [39] Zonghan Wu, Shirui Pan, Guodong Long, Jing Jiang, and Chengqi Zhang. 2019. Graph WaveNet for Deep Spatial-Temporal Graph Modeling. In *Proceedings of the 28th International Joint Conference on Artificial Intelligence*. Macao, China, 1907–1913.
- [40] Qiantong Xu, Gao Huang, Yang Yuan, Chuan Guo, Yu Sun, Felix Wu, and Kilian Q. Weinberger. 2018. An Empirical Study on Evaluation Metrics of Generative Adversarial Networks. *arXiv preprint abs/1806.07755* (2018).
- [41] Jinsung Yoon, James Jordon, and Mihaela van der Schaar. 2018. GAIN: Missing Data Imputation using Generative Adversarial Nets. In *Proceedings of the 35th International Conference on Machine Learning*. Stockholmssmassan, Sweden, 5675–5684.
- [42] Bing Yu, Haoteng Yin, and Zhanxing Zhu. 2018. Spatio-Temporal Graph Convolutional Networks: A Deep Learning Framework for Traffic Forecasting. In *Proceedings of the 27th International Joint Conference on Artificial Intelligence*. Stockholm, Sweden, 3634–3640.
- [43] Junbo Zhang, Yu Zheng, and Dekang Qi. 2017. Deep Spatio-Temporal Residual Networks for Citywide Crowd Flows Prediction. In *Proceedings of the 31st AAAI Conference on Artificial Intelligence*. San Francisco, USA, 1655–1661.
- [44] Weida Zhong, Qiuling Suo, Xiaowei Jia, Aidong Zhang, and Lu Su. 2021. Heterogeneous Spatio-Temporal Graph Convolution Network for Traffic Forecasting with Missing Values. In *41st IEEE International Conference on Distributed Computing Systems*. Virtual Event, 707–717.